

A mechanistic investigation of mechanochromic luminescent organoboron materials†

Xingxing Sun, Xuepeng Zhang, Xinyang Li, Shiyong Liu* and Guoqing Zhang*

Received 4th May 2012, Accepted 3rd July 2012

DOI: 10.1039/c2jm32809g

Mechanochromic luminescence (ML) refers to the luminescence color and/or intensity change of solid-state materials induced by mechanical perturbations. For organic molecular solids, this phenomenon is related to the specific packing modes and orientations of individual fluorophores, which could give rise to different excited-state interactions. The molecular solids of difluoroboron dibenzoylmethane (BF₂dbm) derivatives were previously found to exhibit reversible ML at room temperature and are promising as self-healing optical materials. In this report, we aim to shed some light on the mechanism of BF₂dbm ML by trying to understand the excited-state interactions among solid-state BF₂dbm molecules and elucidate how these interactions change upon mechanical stimulation. We first investigated the optical properties of monomeric, dimeric, and polymeric BF₂dbm derivatives in optically dilute solutions and demonstrated unambiguously that BF₂dbm moieties have a propensity to form H-aggregates. Next, we studied the physical properties of these boron complexes in the solid state including their crystal structures, fluorescence emissions, and mechanochromic luminescence. By correlating solution data with the solid-state characterization results, it was concluded that two coupled processes, force-induced emissive H-aggregate formation and energy transfer to the emissive H-aggregates, are responsible for the observed BF₂dbm ML in the solid state.

1. Introduction

For organic molecular materials, the organization of the building blocks through non-covalent bonds determines the macroscopic properties of such systems.^{1,2} A classical example is the formation of J- and H-aggregates, where blue- and red-shifts in absorption spectra are caused by a mere variation in the slippage angle of the same stacked molecules.³ When external stimuli are introduced, it is possible to switch the molecular organization from one form to another.⁴ As reported by Yi and co-workers,⁵ the hydrophobicity of a naphthylimide-cholesterol coating may be altered by ultrasonic irradiation, resulting from the so called T-gel to S-gel phase transition. This apparent water repellency change occurs due to the adoption of a new preferential bonding mode at the molecular level. As the most fundamental power source, mechanical force may also be employed to harness new properties from molecular assemblies.⁴ For example, mechanically changing the molecular organization of fluorescent species can

generate a drastic alteration in the emission color and/or intensity, which is one of the known causes for piezochromic or mechanochromic luminescence (ML).⁶ Other mechanisms of mechanochromism may involve breakage of covalent bonds such as the force-activated spiropyran to merocyanine reaction.⁷

Studies on ML not only concern apparent applications such as monitoring material deformation and stress,⁸ but also help in the understanding of excited-state interactions which are important for optoelectronics and solar energy research.⁹ In the past few years, many ML molecules have been reported based on chemically distinct core structures.¹⁰ The advantage of molecular ML materials is that their response typically does not involve the breaking of chemical bonds and is therefore reversible, by thermal or solvent treatment in many cases. This allows for repeated application of force and makes them useful fluorescent responsive materials. For example, one of the early studies based on gold(I) thiouracilate complexes, reported by Eisenberg,^{10a} that mechanically induced an intense emission could be attributed to the change in aurophilic interactions. Also based on Au complexes, Ito and coworkers^{10d} reported that the fluorescence emission of (C₆F₅Au)₂(μ-1,4-diisocyanobenzene) complexes turns from blue to yellow upon grinding and the ML process can be reversed by solvent treatment. Pure organic ML materials were previously reported by Sagara and Kato,^{10k} who synthesized liquid crystals with polyaromatic hydrocarbon cores such as pyrene or anthracene. The emission intensity and color of these solid state molecular ensembles can be conveniently tuned

CAS Key Laboratory of Soft Matter Chemistry, Department of Polymer Science and Engineering, University of Science and Technology of China, 96 Jinzhai Road, Hefei, 230026, China. E-mail: gzhang@ustc.edu.cn; sliu@ustc.edu.cn; Fax: +86 551 3606607; Tel: +86 551 3606607

† Electronic supplementary information (ESI) available: Experimental details, characterization methods, and all relevant characterization data are described. CCDC reference numbers 880808–880810. For ESI and crystallographic data in CIF or other electronic format see DOI: 10.1039/c2jm32809g

by mechanical force and heating to achieve dual-colored or even tri-colored luminescence.

Organoboron compounds¹¹ are also of particular interest as fluorescent materials. With potential commercial relevance, a boron-sunscreen complex difluoroboron avobenzene (BF₂AVB) was demonstrated to possess reversible ML with a dramatic emission color change from green-blue to yellow under shear force.¹² The original green-blue fluorescence can be restored by simple thermal treatment. It was found later that many of the difluoroboron dibenzoylmethane (BF₂dbm) derivatives can exhibit ML in the solid state.¹³ However, no conclusive mechanisms were provided given the difficulty in interpreting solid-state spectra, which are highly prone to self-absorption and light scattering.¹⁴ In this article, we attempted to conduct a thorough investigation of the BF₂dbm ML mechanism: when the BF₂dbm crystals/solids are subjected to mechanical force, what and how relevant processes are involved in changing the emission color?

To answer this question, one must first understand the excited-state interactions among BF₂dbm moieties in the solid state. Experimentally, a common strategy to circumvent self-absorption and scattering from solid-state samples would be to spatially confine two or more fluorophores and study the photophysical properties of these confinements in dilute solution. Using covalently linked dimers is a popular strategy since it is simple to work with.¹⁵ However, dimers do not fully reflect the complex environment of the solid state samples, especially after mechanical force application. Polymers, on the other hand, can serve as a bridge from dimers to solid-state systems.¹⁶ Polymers can be molecularly dissolved in solution and unambiguous optical spectra can be obtained. They can also be fabricated into nanoparticles, which are solid-state in nature but can be largely immune to self-absorption and light scattering as well.¹⁷ In this study we shall employ both solution and nanoparticle dispersion of BF₂dbm-containing polymers to help identify the excited-state interactions among BF₂dbm dyes in the solid state.

To study the dynamic process of ML, one must also elucidate the excited-state interactions before and after mechanical stimulation. Crystal structures of BF₂dbm monomers can help predict excited-state information prior to force application. (To avoid confusion with polymer chemistry, the term “monomer” in this study refers to the complex with a single BF₂dbm moiety.) By correlating information obtained from BF₂dbm randomly orientated polymeric aggregates (*e.g.*, nanoparticle dispersion), post-mechanical-force interactions can be inferred since initially

ordered crystals tend to become amorphous based on previous studies.^{10,12,13} Shown below, BF₂dbm complexes **1–3**, **D1**, and **P1** are the monomeric, dimeric, and polymeric derivatives chosen as the model system in the present study.

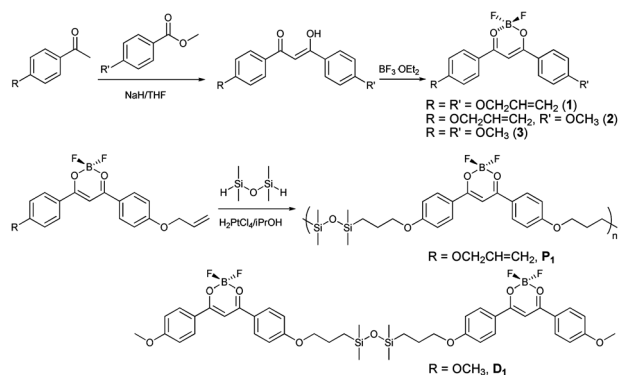
2. Results

2.1 Synthesis

The syntheses of all three monomeric BF₂dbm derivatives are similar, as shown in Scheme 1, by using methoxy- and allyloxy-substituted acetophenones and methyl benzoates. The ketone and ester pairs are refluxed in dry THF for ~48 h to yield the corresponding diketones, which are then chelated with boron trifluoride in CH₂Cl₂ at room temperature to afford bright green-yellow crystals **1–3** after recrystallization from CH₂Cl₂-*n*-hexane. The purity and composition of the products were verified with ¹H NMR and HRMS, respectively (ESI[†]). To prepare the linked dimer **D1** and polymer **P1**, polycondensation reaction was carried out in toluene at ~105 °C under N₂. Hydrosilylations of the boron dye and 1,1,3,3-tetramethyldisiloxane (TMDS) at 2 : 1 and stoichiometric ratios for **D1** and **P1**, respectively, were catalyzed by H₂PtCl₄ (0.05%). **D1** was purified by silica gel chromatography and was verified by ¹H NMR and HRMS. For **P1**, the resulting gummy solid resulting from toluene evaporation was re-dissolved in CH₂Cl₂ for methanol precipitation to remove the monomer and catalyst. The final polymer precipitate was obtained as a yellow powder. **P1** was first examined with ¹H NMR spectroscopy in CDCl₃, and the characteristic vinyl proton resonance peaks usually found at around 6.05 and 5.40 had completely disappeared, instead the methylene proton signal at 0.62 (CH₂-Si) was observed. No peak at ~17 ppm (enol proton of the diketone) was seen, confirming that the methanol precipitation process did not cleave the boron complex to form a diketone, as BF₂bdk complexes are conditionally sensitive towards protic solvents.¹⁸ The polymer molecular weight was determined by GPC (*M*_n = 11 900 Da, PDI = 3.80), showing a broad distribution typical of polycondensation/hydrosilylation reactions.

2.2 Optical characterization in solution state

In dilute CH₂Cl₂, complexes **1–3** exhibit almost identical absorption spectra (λ_{\max} = 412 nm, Fig. 1) characteristic of



Scheme 1

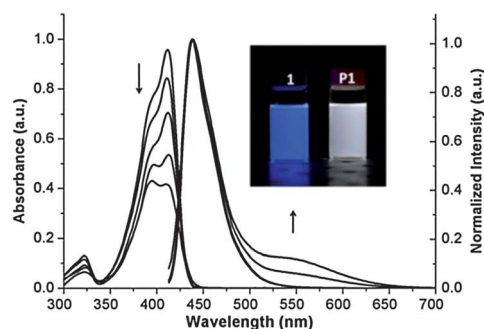


Fig. 1 Absorption and normalized emission spectra of the boron complexes, indicated by the arrows in the order of **1–3**, dimer **D1**, and polymer **P1** in CH₂Cl₂. Inset: photo showing the deep blue and white fluorescence emission of **1** (left) and **P1** (right) in dilute CH₂Cl₂ under UV excitation (λ_{ex} = 365 nm).

strong π - π^* transitions ($\epsilon_{\text{max}} \sim 8 \times 10^4 \text{ M}^{-1} \text{ cm}^{-1}$). For the BF_2dbm dimer **D1**, the absorption maximum remains the same as those of **1–3**, varying only in the relative intensity of a shoulder at $\sim 390 \text{ nm}$. The BF_2dbm -containing polymer **P1** however, exhibits a blue-shifted absorption maximum at 391 nm in addition to the 412 nm peak. The steady-state emission spectra for all the boron complexes were also collected in CH_2Cl_2 (Fig. 1). As expected, **1–3** have almost indistinguishable spectra mostly in the blue region ($\lambda_{\text{em}} = 437 \text{ nm}$, $\Phi_{\text{F}} = 0.93, 0.90, 0.95$ for **1–3**). For **D1** and **P1** however, despite their unaltered emission maxima at 437 nm , an additional lower energy shoulder was observed at around 550 nm . As a result, unlike the deep blue emission from monomer **1**, the dilute solution of polymer **P1** in CH_2Cl_2 exhibits a white-colored photoluminescence (PL) to the naked eye under UV irradiation (Fig. 1 inset). The excitation spectra monitored at 550 nm for **D1** and **P1** are also distinctly different from that monitored at 440 nm (Fig. S1 and S2†): for both **D1** and **P1**, the blue-shifted absorption at 391 nm results in emission at 550 nm but a red-shifted absorption at 412 nm corresponds to fluorescence emission at a much shorter wavelength (437 nm).

Fluorescence lifetimes of these boron complexes in CH_2Cl_2 were measured as well. **1–3** have almost the same single-exponential decay of $\sim 1.68 \text{ ns}$. Although the emission band at 437 nm of **D1** and **P1** can almost overlap with those of **1–3**, the fluorescence decay profiles of **D1** and **P1** at 440 nm are quite different. **D1** has a pseudo single-exponential decay of 1.34 ns but **P1** is fitted to a triple-exponential decay with a pre-exponential averaged value of 1.29 ns . When monitored at 550 nm , the lifetime of **D1** and **P1** (39 and 40 ns) is much longer.

2.3 Optical characterization of the P1 nanoparticle dispersion

We also investigated the photophysics of BF_2dbm dye aggregates in the form of nanoparticles so that optical distortions remain non-problematic while its solid-state properties are retained. As a result, the investigation of the nanoparticles links the solution characterization results to those in the solid state. Polymer **P1** in acetone (BF_2dbm concentration $1 \times 10^{-3} \text{ M}$) was fabricated into polymeric nanoparticles with an intensity-average hydrodynamic diameter of 54.4 nm and a size polydispersity of 0.088 as determined by DLS, (Fig. S3†).¹⁸ The nanoparticle dispersion has a greenish yellow fluorescence emission under UV light and exhibits a Gaussian-shaped emission spectrum ($\lambda_{\text{ex}} = 545 \text{ nm}$).

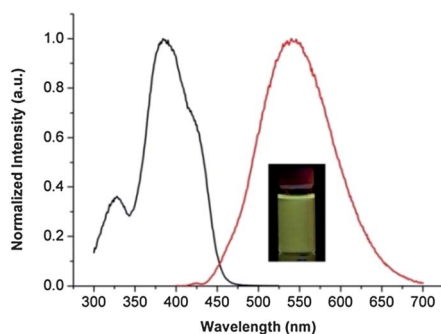


Fig. 2 Normalized excitation and emission spectra of **P1** nanoparticle dispersion in water; inset: photo of the nanoparticle dispersion under UV light ($\lambda_{\text{ex}} = 385 \text{ nm}$, excitation monitored at 550 nm).

When monitored at around the emission maximum (550 nm), the excitation spectrum resembles the absorption of **P1** in CH_2Cl_2 with a slightly more blue-shifted maximum at 384 nm (Fig. 2).

2.4 Crystal structures of monomers 1–3

To seek structure–property relationships of BF_2dbm dyes in the solid state, single crystal XRD measurements were performed. During a period of six months, we were unable to obtain single-crystals for **D1**, probably due to the dynamic nature of the flexible linker and the increased freedom of motion. For complexes **1–3**, upon crystallization, minor difference in the carbon number or saturation of the alkyl chain leads to conspicuous variations in crystal packing. Although **3** is a known compound, crystal structures were solved for all three complexes given this class of molecule has been found to possess multiple polymorphs depending on the crystallization conditions.¹² We did not identify more than one polymorph in this experiment when single crystals were obtained by *n*-hexane diffusion into CH_2Cl_2 at room temperature.

Fig. 3 shows the unit cell packing of each of the three complexes **1–3**. Consistent with previous studies, the BF_2dbm backbones are rather rigid and mostly planar.^{12,19} All three crystals are monoclinic with space groups of C_2/c , P_c , and C_2/c for **1–3**, respectively. The BF_2dbm complexes all adapt to an anti-parallel packing manner (*i.e.*, the BF_2 moiety points to the opposite direction compared to the BF_2 group on the nearest neighbor) and significant π - π stacking is noticed for **1** and **3**. For **3**, the diketone ring lays above the phenyl ring of its nearest neighbor at a distance of 3.54 \AA .

Weak interactions including $\text{ArH}\cdots\text{F}$, $\text{OCH}\cdots\text{F}$, $\text{CH}=\text{CH}\cdots\text{O}$, $\text{CH}\cdots\text{HC}$, $\text{C}=\text{C}\cdots\text{O}$ are identified in these molecular systems (Fig. S4†). Specifically, $\text{ArH}\cdots\text{F}$ interactions occur in a symmetric fashion involving both fluorine atoms on the BF_2 moiety and two hydrogen atoms from the 2 and 2' positions on the phenyl ring in complexes **1** and **3**. The two fluorine hydrogen bonds distances are 2.628 and 2.664 \AA for **1** and **3**, respectively. These fluorine hydrogen bonds alternate between adjacent molecules and propagate along one dimension. For **2** however, one boron molecule directly interacts with eight neighboring molecules (*versus* two in **1** and **3**) through multiple weak interactions ($\text{O}\cdots\text{CH}=\text{CH}$, $\text{CH}\cdots\text{HC}$, $\text{C}=\text{C}\cdots\text{O}$) in addition to $\text{ArH}\cdots\text{F}$ hydrogen bonding, which is the only form of interaction in the case of **1** and **3**. In **2**, only one fluorine is involved and the

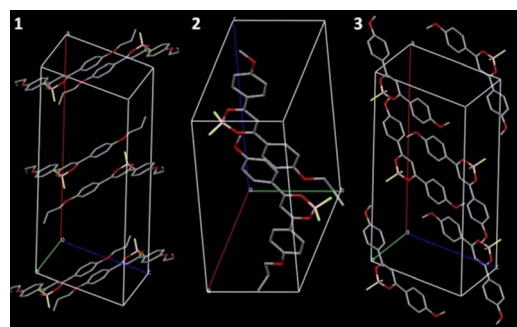


Fig. 3 Illustration of unit cell packing for boron dye single crystals **1–3**. Hydrogen atoms are omitted for clarity.

dual hydrogen bonding ($\text{H}\cdots\text{F}\cdots\text{H}$) consists of one hydrogen atom from the allyloxy group ($\text{ArOCH}\cdots\text{F}$) and the other from the phenyl ring ($\text{ArH}\cdots\text{F}$) (Fig. S4†). They are 2.470 and 2.572 Å away from the fluorine atom, respectively. This combination of interactions causes the allyl group to bend towards the contacting fluorine atom and increases the B–F bond by 0.033 Å compared to the other B–F bond (that does not participate) and by 0.025 Å compared to the B–F bond in **1** (that forms a mono $\text{ArH}\cdots\text{F}$ contact). Detailed crystal data are also provided (ESI, Tables S1–S21†).

2.5 Photophysical properties in the solid state

Given that most BF_2dbm derivatives exhibit reversible ML,^{12,13} namely that their emission spectra spontaneously recover over time after mechanical perturbation, it is problematic to record ML spectra on a FluoroMax spectrometer since collecting a decent emission spectrum typically takes 3–5 min over the visible range while many BF_2dbm dyes have ML recovery timeframes shorter than a few minutes.¹³ To solve this problem, an optical fiber attached to a linear CCD-array spectrometer with 25 ms integration time equipped with a built-in LED excitation module ($\lambda_{\text{ex}} = 385 \text{ nm}$) was mounted to the sample holder of a fluorescence microscope. In this setup, fluorescence micrographs

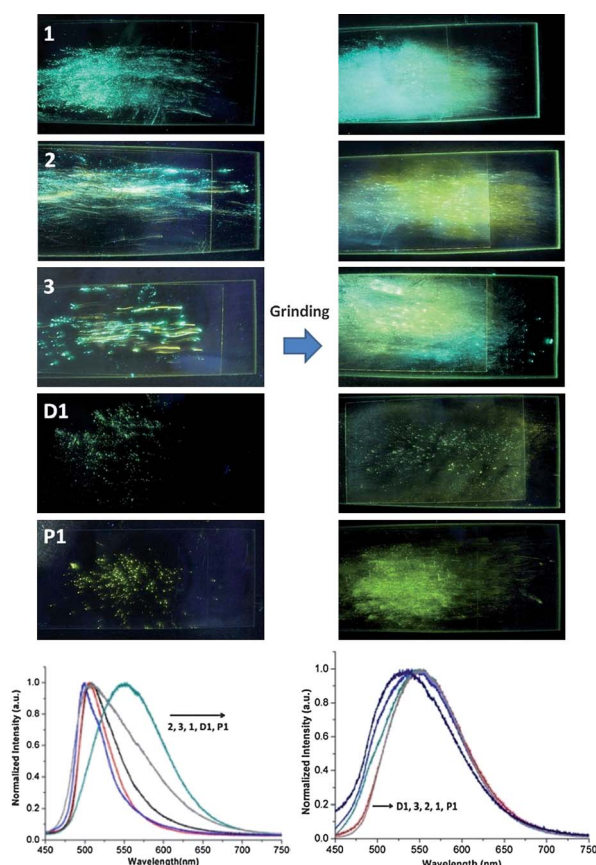


Fig. 4 Photos of **1–3**, **D1**, and **P1** solids on microscope slides with glass covers under UV light. Left: the solids were gently moved by the glass covers; right: the solids were repeatedly pressed hard. The plots at the bottom show the emission spectra of each solid before (left) and after hard pressing (right).

and their corresponding spectra in small regions could be obtained simultaneously, minimizing sample heterogeneity problems. In this section, to avoid problems associated with instrumentation discrepancy, all fluorescence spectra were recorded with the array spectrometer.

Under a fluorescence microscope ($\lambda_{\text{ex}} = 405 \text{ nm}$), needle-shaped, sheet-like, and thick needle crystalline species were observed for **1–3**, respectively (Fig. S5†). The dimer **D1** appeared as an irregular polycrystalline solid. Among complexes **1–3**, the single crystals of complex **2** exhibit the most narrow and blue-shifted fluorescence emission ($\lambda_{\text{max}} = 500 \text{ nm}$, $\tau_{\text{F}} = 1.54 \text{ ns}$, Fig. 4) compared to **1** ($\lambda_{\text{max}} = 505 \text{ nm}$, $\tau_{\text{F}} = 4.35 \text{ ns}$) and **3** ($\lambda_{\text{max}} = 509 \text{ nm}$, $\tau_{\text{F}} = 2.87 \text{ ns}$), whose spectra are red-shifted and broadened in the lower energy region. The polymer solids have a broad and structureless spectrum at 554 nm ($\tau_{\text{F}} = 24.2 \text{ ns}$) while that of the dimer solids ($\lambda_{\text{max}} = 511 \text{ nm}$, $\tau_{\text{F}} = 8.92 \text{ ns}$) is an intermediate between the monomers and the polymer.

2.6 Mechanochromic luminescence

Like many BF_2dbm derivatives, ML was observed in **1–3** and **D1** (Fig. 4 photos). When the crystals of **1–3** and solid **D1** were sandwiched between microscope glass slides and covers, **2** and **3** left bright yellow streaks and cover slips upon the very gentle sliding of the thin covers ($\sim 500 \text{ mg}$ in weight), demonstrating high sensitivity towards mechanical force. On the other hand, **1** and **D1** did not exhibit ML until the solids were pressed very firmly and sheared in between the two pieces of glass. Although the roles of the substituents and substrates on ML are not within the scope of this study, clearly the substituent effects, which are practically non-existent in dilute solution, are once again manifested in the solid state. The polymer **P1** did not show any visual fluorescence color or intensity change after being ground against the substrate with substantial shear force.

The photos, fluorescence micrographs, emission spectra and fluorescence lifetimes (collected and averaged over $\sim 2 \text{ min}$) were recorded for the solid smears. After hard pressing, the crystals were mostly amorphous under the microscope (Fig. S5†). Their emission spectra were instantly recorded by the array spectrometer. Unlike the relatively narrow fluorescence emission found in the crystalline state, the smeared solids all exhibit similar Gaussian-shaped spectra (Fig. 4). The fluorescence lifetimes for the smears (**1–3** and **D1**) range from 7–10 ns with fluctuations due to the spontaneous morphological changes of



Fig. 5 (a) Reversible ML of **3** loaded on a piece of weighing paper: writing “Exciton Migration” with a wood stick and erasing it by heating at 120 °C for 30 s; (b) quickly dimmed ML of **1** after shear force and brightness restoration by repeated smearing with a cotton swab on the areas sheared $\sim 15 \text{ s}$ ago. ($\lambda_{\text{ex}} = 365 \text{ nm}$).

the solid samples.^{12,13} It was interesting to see that irrespective of the initial emissions, all the samples ended up with similar spectra after being ground *via* mechanical force, suggesting similar amorphous states for all molecules.

Consistent with previous studies,^{12,13} the ML of **1–3** and **D1** is reversible, namely that the yellow ML spontaneously reverts to the blue-green. This process takes longer at room temperature but can be substantially expedited at 120 °C, which is still well below the melting temperatures of these solids (>185 °C). The reversibility was demonstrated with **3** on a piece of weighing paper as shown in Fig. 5a. Again, details of the substituent and substrate effects are not discussed in the current study. A previously unnoticed interesting feature of BF₂dbm ML is that the freshly sheared sites tend to become dimmer very quickly (extended time leads to color change) but the brightness can be reinstated by repeated shear force (Fig. 5b). In this process however, the emission color is not altered, only the intensity is.

3. Discussion

3.1 Excited state interactions among BF₂dbm(OR)₂

From characterization in dilute CH₂Cl₂, it is clearly evident that when BF₂dbm moieties are spatially constrained (**D1** and **P1**), intermolecular interactions give rise to a new emission band (~550 nm) that is absent when the dye molecules are discrete (**1–3**). There are two common causes for a red-shifted fluorescence band for proximal dyes of the same species: excited-state or ground-state dimers. Excited-state dimers are also known as excimers,²⁰ which are only attractive to each other in the excited state but are non-interacting or repulsive in the ground state. Thus excimers absorb light as discrete molecules and emit light as associated ones. Ground-state dimers however, can be excited by light as one delocalized entity which differs in transition energy to the monomer and results in new absorption bands.²¹

From absorption data obtained for **1–3**, **D1** and **P1** in solution and nanoparticle dispersion of **P1**, we are quite convinced that BF₂dbm dyes have a strong tendency to form ground-state dimers for the reason mentioned above. A blue-shifted absorption band at 391 nm is responsible for the new fluorescence band at ~550 nm for **D1** and **P1** (Fig. S1 and S2†). This hypsochromic dimer, or H-dimer (H-aggregate) is formed when two (or more) dye molecules are arranged in “face-to-face” configurations.²¹ Although the absorption evidence is not clear enough for **D1**, it is possible that the intramolecular H-dimer²² and the unassociated counterpart are at equilibrium in solution.²³ Presumably the enthalpy-driven ground-state dimer prefers less polar solvents, due to the large dipoles²⁴ and multiple non-covalent interactions of BF₂dbm solute molecules (inferred from crystal structures, Fig. S4†). It is expected to see increased dimer probability (population) when the solvent polarity is decreased. Fig. 6a shows the **D1** absorption (5.6×10^{-6} M) change in response to decreased solvent polarity, where a CH₂Cl₂–*n*-hexane mixture at various volume ratios is used as the solvent. When the content of polar CH₂Cl₂ decreases, not only does the absorption show a blue shift, the intensity of the absorption maximum also increases by more than 50% in pure CH₂Cl₂ compared to 9 : 1 *n*-hexane–CH₂Cl₂. The increase in the new absorption band is presumably due to aligned transition dipole moments of the two

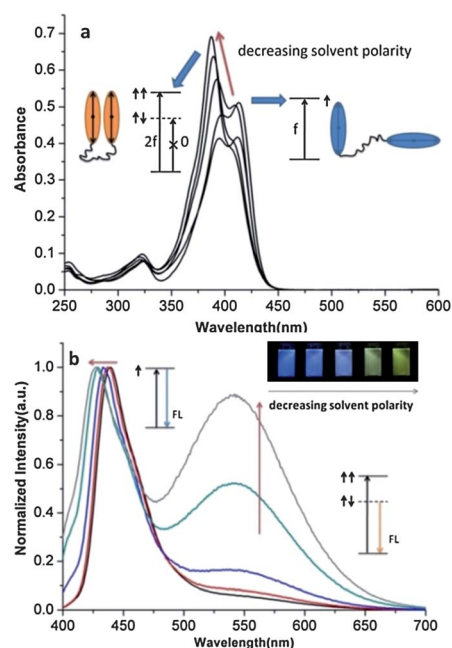


Fig. 6 (a) Absorption spectra of **D1** in a mixture of CH₂Cl₂ and *n*-hexane with different CH₂Cl₂ content percentages: 100%, 80%, 50%, 20%, and 10% at a fixed concentration of 5.6×10^{-6} M. Inset: schematic representation of increased transition probability at higher energy level of the BF₂dbm H-dimer with “face-to-face” parallel transition dipoles. The strength of the transition is denoted with “*f*” (oscillator strength²¹). Black arrows denote the transition dipole moments. Solid and dotted lines denote allowed and forbidden excited states.²¹ (b) Normalized steady-state emission spectra of **D1** in a mixture of CH₂Cl₂ and *n*-hexane with different CH₂Cl₂ content percentages: 100%, 80%, 50%, 20%, and 10% at a fixed concentration of 5.6×10^{-6} M ($\lambda_{\text{ex}} = 385$ nm). Inset: corresponding photos of the five samples under UV light and schematic presentation of monomer and H-dimer fluorescence (FL).

BF₂dbm moieties in the “face-to-face” configuration (Fig. 6a inset). Meanwhile, the fluorescence emission contributed by the emissive H-dimer (~550 nm, $\tau_{\text{F}} = 39$ ns) is boosted with diminished solvent polarity (Fig. 6b). The red-shifted and long-lived fluorescence is also typical of an H-dimer due to cancelled transition dipoles in a lower energy state (Fig. 6b inset). The absorption spectra of **1** in decreasing polarity solvents were measured in addition to a control experiment (Fig. S6†). Although the absorption maximum of **1** shows a slight blue-shift (412 to 403 nm), neither the shape nor the intensity of the absorption shows a perceivable change, indicating that the blue-shift is merely a result of the solvatochromic effect. The mild solvatochromic effect was observed in the fluorescence emission of **1** too with no additional band for the various solvent polarities (Fig. S6†).

For the polymer **P1**, higher-ordered H-aggregates are possible since from Fig. 1, **P1** exhibits a more dramatic blue-shifted absorption and a greater contribution from low energy emission than does **D1**. The alternating polar, rigid fluorophores and non-polar, flexible linkers could allow for intrapolymer H-aggregate formation.^{25,26} The equally long-lived lifetime of **P1** (40 ns) is also characteristic of H-aggregate emission. Although impurities, defects, excimers, and exciplexes which all render red-shifted emissions are not uncommon in conjugated fluorescent

polymers,²⁷ **P1** is essentially a site-isolated system and is thus far less complicated to study than conjugated systems. Therefore, these solution experiments unambiguously demonstrated the propensity of H-aggregate, formation by BF₂dbm dyes.

The excitation spectrum of the NPs in water reveals a further blue-shifted maximum relative to that of the monomers **1–3** (Fig. 4, from 411 nm to 384 nm, or 1770 cm⁻¹), which indicates that the same type, but possibly stronger, H-aggregate association occurs in more firmly packed BF₂dbm dye clusters. Thus the NPs fluorescence emission (~550 nm, τ_F = 24 ns) that closely matches the lower energy part of **D1** and **P1** (~550 nm) in solution is most likely to be caused by emissive H-aggregates as well. The shorter fluorescence lifetime of the NP (compared to 40 ns of the H-aggregates in CH₂Cl₂) is possibly caused by increased quenching events in the solid state. Since the polymer particle (highly spatially confined and yet with rotationally flexible linkers) is a close mimic of amorphous BF₂dbm solids, we have a good reason to believe the red-shifted emission (~550 nm) induced by mechanical force in **1–3** is also caused by the formation of H-aggregates. As for the tendency for dimer or aggregate formation in the solid state of BF₂dbm derivatives, in previous and our current investigations, both single-crystal XRD^{12,19} and STM²⁸ studies reveal that π–π stacking and ArH...F hydrogen bonding could both contribute significantly.

3.2 Energy transfer in the solid state

Since the orientations of BF₂dbm moieties in polymer solids and sheared crystals are more likely to be random, with the possibility to form site-isolated BF₂dbm fluorophores and J-aggregate-like structures, one obvious question to ask is why only H-aggregates emission is observed? Or how is it possible to achieve uniform fluorescence color conversion with crude mechanical stimuli, as has been observed in the experiments? A hypothesis is that (unperturbed) ordered crystals and other dye–dye interactions possess higher excited state energy levels than those of the emissive H-aggregates, which serve as acceptors (traps) in energy transfer.^{29,30} Given that some energy transfer events (or exciton migration³¹ in this case) can be thermally activated,³² it is expected that BF₂dbm ML can be quite different at lower temperatures.

Indeed when the glass slide covered with smeared solid of **3** was bathed in liquid N₂ (Fig. 7), it was clearly visible that the originally homogeneous yellow emission turned into three different apparent colors (cyan, green, and yellow) readily observable to the naked eye. The heavily smeared regions were more yellow while the less smeared parts changed to cyan or green emission. Similar observations were noted for **1** and **2** (not

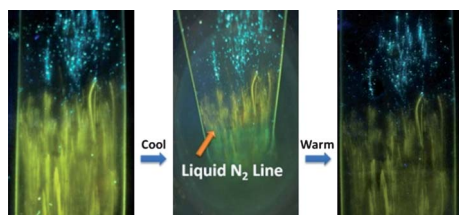


Fig. 7 Photos showing ML manifested by smearing crystals of **3** on glass at room temperature (left), bottom part of the smeared region bathed in liquid N₂ (middle), and recovery of ML when the glass slide was retrieved from liquid N₂ to warm up to room temperature. (λ_{ex} = 365 nm).

shown). It was noted that neither at room temperature nor at 77 K did the smeared region exhibit maximal ML effect; it was a temperature region in between. The simple experiments have convincingly demonstrated the temperature-dependent energy transfer processes within the solid organoboron materials.

Previous studies also confirm that H-aggregate-like structure of BF₂dbm derivatives have the lowest emissive states: the only known BF₂dbm derivative that does not show ML is a single-methoxy substituted (Fig. 8). The dye, BF₂dbmOME, was used to monitor bulk polymerization of lactide because of its robust crystalline emission at ~550 nm (τ_F = 41 ns),³³ which coincides with the spectra of the sheared crystals of **1–3**, **D1** and the NP and solids of polymer **P1**. Unsurprisingly, the solved crystal structure¹⁹ of BF₂dbmOME reveals a fully overlapped “face-to-face” H-aggregate-like packing mode which is absent in any other BF₂dbm derivatives studied, including the current crystal structures for **1–3**. As a result, the energy levels cannot be brought down further by mechanical stimulation. Nonetheless, a more symmetric spectrum was noted after grinding, which either could be caused by reduced self-absorption or increased chaos in the molecular orientations caused by mechanical force.

To confirm that the yellow emission from BF₂dbmOME mostly comes from stable H-aggregates and the effect of exciton migration is minor in this case, smeared crystals of BF₂dbmOME were bathed in liquid N₂ under UV light. Unlike **1–3** the smeared crystals of which show blue-shifted emission at 77 K, BF₂dbmOME turns orange with a second-long, red “after-glow” after the UV excitation had ceased (Fig. 8 inset). This is a clear indication of strong phosphorescence, or triplet-state emission from the H-aggregates. As has been explained in the insets of Fig. 6a and b, H-aggregates have a forbidden (long-lived) lowest singlet state (τ_F = 40 ns), which significantly enhances the probability of intersystem crossing to triplet states.²¹ Therefore, it is not surprising to see red-shifted emission from BF₂dbmOME solids and not from **1–3**. This is because the H-aggregate population generated by mechanical force for **1–3** could be small and does not result in detectable phosphorescence.

3.3 A mechanistic model for BF₂dbm ML in the solid state

Based on the experimental data in the current and previous studies, we have summarized a mechanistic explanation for the

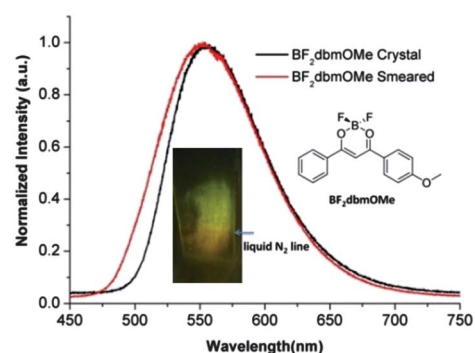


Fig. 8 Fluorescence emission spectra of crystals and smeared crystals of BF₂dbmOME on glass substrates (λ_{ex} = 385 nm). Inset: chemical structure of BF₂dbmOME and photo showing smeared BF₂dbmOME crystals partially bathed in liquid N₂ under UV light. (λ_{ex} = 365 nm).

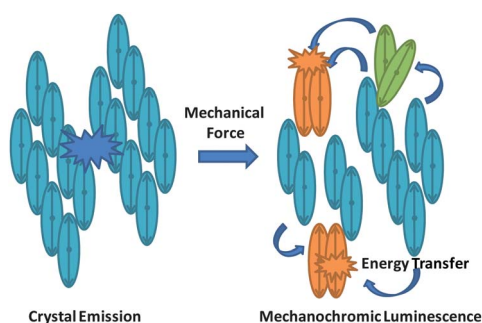


Fig. 9 Pictorial representation of BF₂dbm ML process: the crystals are ordered and emit green-blue fluorescence (blue molecules); when the order is disrupted by mechanical force, limited numbers of H-aggregate-forming sites (orange molecules) can give the entire solid a red-shifted emission mediated by energy transfer (exciton migration). Green molecules in the Fig. represent any other type of intermolecular interaction with an excited-state energy level above that of the H-aggregates but below the crystals.

BF₂dbm ML phenomenon shown in Fig. 9. Before mechanical stimulation, the emission color (energy level) of the BF₂dbm crystals is determined by the manner of molecular packing in crystals (hypothetically, green-blue in the scheme).³⁴ Nonetheless, irrespective of the starting emissive energy levels of the crystals, after shear force is applied, the ordered state is disrupted into randomness and all possible dye–dye interactions can be adopted, which could give rise to many non-vanishing excited states.³⁵ Among the many dye–dye interactions, shear force could always bring about the possibility of H-aggregate-like association (a metastable state), which has the lowest emissive energy level and serves as the acceptor in efficient solid-state energy transfer. Therefore exciton migration can happen from other allowed states (resulted from different dye–dye interactions) to H-aggregate emissive states.

The proposed model predicts that for BF₂dbm derivatives, different solids with different starting fluorescence emission colors will end in the same, lowest emissive state (specifically ~550 nm) after mechanical stimulation, provided that H-aggregates are not highly unfavorable. That is to say that BF₂dbm ML should be dependent on the Gibbs free energy for H-aggregate formation in the ground state. If the free energy is negative, BF₂dbm H-aggregates are stable and thus no ML, in terms of emission color change, should be observed (Fig. 8). This is the case of BF₂dbmOMe which has an H-aggregate-like crystal structure. If the free energy is positive, ML should be observable since the initial stable packing mode differs from the metastable H-aggregates. This is the case for the majority of the crystals and solids observed.

4. Conclusions

In summary, we have synthesized monomeric, dimeric and polymeric derivatives of difluoroboron dibenzoylmethane (BF₂dbm) complexes to investigate the mechanism of the mechanochromic luminescence exhibited by most BF₂dbm complexes in the solid state. Using an approach that allows us to unambiguously obtain excited-state interactions among BF₂dbm fluorophores, we were able to conclude the following statements:

(1) BF₂dbm fluorophores have a propensity to form H-dimers or H-aggregates in solution and in amorphous solids, such as polymeric nanoparticles or smeared BF₂dbm crystals; (2) mechanical stimuli can cause the formation of the H-dimers or H-aggregates of BF₂dbm that exhibit a low-lying emissive state around 550 nm; (3) energy transfer may happen from other higher excited states to the lowest H-aggregate excited states, which eventually makes the entire solid emit at ~550 nm. This investigation can serve as a guideline for tailored material design in the future.

Acknowledgements

The work was supported by the University of Science and Technology of China startup funds and the National Natural Science Foundation of China (J1030412). We also thank Mr Joshua Vaughn for the photos.

Notes and references

- G. M. Whitesides, E. E. Simanek, J. P. Mathias, C. T. Seto, D. Chin, M. Mammen and D. M. Gordon, *Acc. Chem. Res.*, 1995, **28**, 37.
- J. A. A. W. Elemans, A. E. Rowan and R. J. M. Nolte, *J. Mater. Chem.*, 2003, **13**, 2661–2670.
- J. Seo, S. Kim, S. H. Gihm, C. R. Park and S. Y. Park, *J. Mater. Chem.*, 2007, **17**, 5052–5057.
- K. Ariga, T. Mori and J. P. Hill, *Adv. Mater.*, 2012, **24**, 158–176.
- J. Wu, T. Yi, T. Shu, M. Yu, Z. Zhou, M. Xu, Y. Zhou, H. Zhang, J. Han, F. Li and C. Huang, *Angew. Chem., Int. Ed.*, 2008, **47**, 1063–1067.
- (a) The first review in the field: Y. Sagara and T. Kato, *Nat. Chem.*, 2009, **1**, 605–610; (b) L. Maggini and D. Bonifazi, *Chem. Soc. Rev.*, 2012, **41**, 211–241; (c) A thorough and more recent review: Z. Chi, X. Zhang, B. Xu, X. Zhou, C. Ma, Y. Zhang, S. Liu and J. Xu, *Chem. Soc. Rev.*, 2012, **41**, 3878–3896.
- D. A. Davis, A. Hamilton, J. Yang, L. D. Cremar, D. Van Gough, S. L. Potisek, M. T. Ong, P. V. Braun, T. J. Martinez, S. R. White, J. S. Moore and N. R. Sottos, *Nature*, 2009, **459**, 68–72.
- C. Löwe and C. Weder, *Adv. Mater.*, 2002, **14**, 1625–1629.
- (a) S. R. Forrest and M. E. Thompson, *Chem. Rev.*, 2007, **107**, 923–925; (b) Y. Kim, J. Bouffard, S. E. Kooi and T. M. Swager, *J. Am. Chem. Soc.*, 2005, **127**, 13726–13731; (c) S. Kim, J. K. Lee, S. O. Kang, J. Ko, J. H. Yum, S. Fantacci, F. De Angelis, D. Di Censo, M. K. Nazeeruddin and M. Grätzel, *J. Am. Chem. Soc.*, 2006, **128**, 16701–16707; (d) V. Bulović, R. Deshpande, M. E. Thompson and S. R. Forrest, *Chem. Phys. Lett.*, 1999, **308**, 317–322.
- (a) Y.-A. Lee and R. Eisenberg, *J. Am. Chem. Soc.*, 2003, **125**, 7778–7779; (b) J. W. Chung, Y. You, H. S. Huh, B.-K. An, S.-J. Yoon, S. H. Kim, S. W. Lee and S. Y. Park, *J. Am. Chem. Soc.*, 2009, **131**, 8163–8172; (c) C. Dou, L. Han, S. Zhao, H. Zhang and Y. Wang, *J. Phys. Chem. Lett.*, 2011, **2**, 666–670; (d) H. Ito, T. Saito, N. Oshima, N. Kitamura, S. Ishizaka, Y. Hinatsu, M. Wakeshima, M. Kato, K. Tsuge and M. Sawamura, *J. Am. Chem. Soc.*, 2008, **130**, 10044–10045; (e) H. Li, X. Zhang, Z. Chi, B. Xu, W. Zhou, S. Liu, Y. Zhang and J. Xu, *Org. Lett.*, 2011, **13**, 556–559; (f) X. Luo, J. Li, C. Li, L. Heng, Y. Q. Dong, Z. Liu, Z. Bo and B. Z. Tang, *Adv. Mater.*, 2011, **23**, 3261–3265; (g) J. Ni, X. Zhang, N. Qiu, Y.-H. Wu, L.-Y. Zhang, J. Zhang and Z.-N. Chen, *Inorg. Chem.*, 2011, **50**, 9090–9096; (h) Y. Ooyama and Y. Harima, *J. Mater. Chem.*, 2011, **21**, 8372–8380; (i) A. Pucci and G. Ruggeri, *J. Mater. Chem.*, 2011, **21**, 8282–8291; (j) D. R. T. Roberts and S. J. Holder, *J. Mater. Chem.*, 2011, **21**, 8256–8268; (k) Y. Sagara and T. Kato, *Angew. Chem.*, 2011, **123**, 9294–9298; (l) S.-J. Yoon, J. W. Chung, J. Gierschner, K. S. Kim, M.-G. Choi, D. Kim and S. Y. Park, *J. Am. Chem. Soc.*, 2010, **132**, 13675–13683; (m) A. L. Balch, *Angew. Chem., Int. Ed.*, 2009, **48**, 2641–2644; (n) S.-J. Yoon and S. Park, *J. Mater. Chem.*, 2011, **21**, 8338–8346; (o) J. Mei, J. Wang, A. Qin, H. Zhao, W. Yuan, Z. Zhao, H. H. Y. Sung, C. Deng, S. Zhang, I. D. Williams, J. Z. Sun and

- B. Z. Tang, *J. Mater. Chem.*, 2012, **22**, 4290–4298; (p) S. Perruchas, X. F. L. Goff, S. B. Maron, I. Maurin, F. O. Guillen, A. Garcia, T. Gacoin and J.-P. Boilot, *J. Am. Chem. Soc.*, 2010, **132**, 10967–10969.
- 11 (a) F. Jäkle, *Chem. Rev.*, 2010, **110**, 3985–4022; (b) Z. M. Hudson and S. Wang, *Acc. Chem. Res.*, 2009, **42**, 1584–1596; (c) A. Nagai, J. Miyake, K. Kokado, Y. Nagata and Y. Chujo, *J. Am. Chem. Soc.*, 2008, **130**, 15276–15278; (d) W. L. Jia, M. J. Moran, Y.-Y. Yuan, Z. H. Lu and S. Wang, *J. Mater. Chem.*, 2005, **15**, 3326–3333.
- 12 G. Zhang, J. Lu, M. Sabat and C. L. Fraser, *J. Am. Chem. Soc.*, 2010, **132**, 2160–2162.
- 13 (a) G. Zhang, J. P. Singer, S. E. Kooi, R. E. Evans, E. L. Thomas and C. L. Fraser, *J. Mater. Chem.*, 2011, **21**, 8295–8299; (b) N. D. Nguyen, G. Zhang, J. Lu, A. E. Sherman and C. L. Fraser, *J. Mater. Chem.*, 2011, **21**, 8409–8415; (c) T. Liu, A. D. Chien, J. Lu, G. Zhang and C. L. Fraser, *J. Mater. Chem.*, 2011, **21**, 8401–8408.
- 14 (a) G. Bourhill, L. O. Pålsson, I. D. W. Samuel, I. C. Sage, I. D. H. Oswald and J. P. Duignan, *Chem. Phys. Lett.*, 2001, **336**, 234–241; (b) M. J. Mayoral, P. Ovejero, M. Cano and G. Orellana, *Dalton Trans.*, 2011, **40**, 377–383.
- 15 (a) C. Curutchet and B. Mennucci, *J. Am. Chem. Soc.*, 2005, **127**, 16733–16744; (b) V. Russo, C. Curutchet and B. Mennucci, *J. Phys. Chem. B*, 2007, **111**, 853–863.
- 16 U. H. F. Bunz, V. Enkelmann, L. Kloppenburg, D. Jones, K. D. Shimizu, J. B. Claridge, H.-C. zur Loye and G. Lieser, *Chem. Mater.*, 1999, **11**, 1416–1424.
- 17 G. Kuzmanich, S. Simoncelli, M. N. Gard, F. Spänig, B. L. Henderson, D. M. Guldi and M. A. Garcia-Garibay, *J. Am. Chem. Soc.*, 2011, **133**, 17296–17306.
- 18 A. Pfister, G. Zhang, J. Zareno, A. F. Horwitz and C. L. Fraser, *ACS Nano*, 2008, **2**, 1252–1258.
- 19 A. G. Mirochnik, B. V. Bukvetskii, E. V. Fedorenko and V. E. Karasev, *Russ. Chem. Bull.*, 2004, **53**, 291–296.
- 20 A. Pucci, F. Di Cuia, F. Signori and G. Ruggeri, *J. Mater. Chem.*, 2007, **17**, 783–790.
- 21 M. Kasha, H. R. Rawls and A. El-Bayoumi, *Pure Appl. Chem.*, 1965, **11**, 371–392.
- 22 F. C. Spano, *Acc. Chem. Res.*, 2009, **43**, 429–439.
- 23 U. Rösch, S. Yao, R. Wortmann and F. Würthner, *Angew. Chem., Int. Ed.*, 2006, **45**, 7026–7030.
- 24 E. Cogné-Laage, J.-F. Allemand, O. Ruel, J.-B. Baudin, V. Croquette, M. Blanchard-Desce and L. Jullien, *Chem.–Eur. J.*, 2004, **10**, 1445–1455.
- 25 M. Kasha, *Radiat. Res.*, 1963, **20**, 55–71.
- 26 T.-Q. Nguyen, V. Doan and B. J. Schwartz, *J. Chem. Phys.*, 1999, **110**, 4068–4078.
- 27 S. A. Jenekhe and J. A. Osaheni, *Science*, 1994, **265**, 765–768.
- 28 (a) X. Zhang, C.-J. Yan, G.-B. Pan, R.-Q. Zhang and L.-J. Wan, *J. Phys. Chem. C*, 2007, **111**, 13851–13854; (b) D. Rohde, C.-J. Yan, H.-J. Yan and L.-J. Wan, *Angew. Chem., Int. Ed.*, 2006, **45**, 3996–4000.
- 29 H. C. Wolf, in *Advances in Atomic and Molecular Physics*, ed. D. R. Bates and E. Immanuel, Academic Press, 1968, vol. 3, pp. 119–142.
- 30 (a) C. E. Evans and P. W. Bohn, *J. Am. Chem. Soc.*, 1993, **115**, 3306–3311; (b) C. W. Farahat, T. L. Penner, A. Ulman and D. G. Whitten, *J. Phys. Chem.*, 1996, **100**, 12616–12623.
- 31 J.-I. Lee, T. Zyung, R. D. Miller, Y. H. Kim, S. C. Jeoung and D. Kim, *J. Mater. Chem.*, 2000, **10**, 1547–1550.
- 32 D. Beljonne, G. Pourtois, C. Silva, E. Hennebicq, L. M. Herz, R. H. Friend, G. D. Scholes, S. Setayesh, K. Müllen and J. L. Brédas, *Proc. Natl. Acad. Sci. U. S. A.*, 2002, **99**, 10982–10987.
- 33 G. Zhang, S. Xu, A. G. Zestos, R. E. Evans, J. Lu and C. L. Fraser, *ACS Appl. Mater. Interfaces*, 2010, **2**, 3069–3074.
- 34 M. Schwoerer and H. C. Wolf, in *Organic Molecular Solids*, Wiley-VCH Verlag GmbH, 2008, pp. 125–175.
- 35 G. D. Scholes and G. Rumbles, *Nat. Mater.*, 2006, **5**, 683–696.